 doi:10.20944/preprints202103.0242.v1

Article

Genomic Fabric Remodeling in Prostate Cancer

Sanda Iacobas [1], Dumitru A Iacobas [1,*]

1 Department of Pathology, New York Medical College, Valhalla, NY 10595, U.S.A.
2 Personalized Genomics Laboratory, Center for Computational Systems Biology, Roy G Perry College of Engineering, Prairie View A&M University, Prairie View, TX 77446, U.S.A.
* Correspondence: daiacobas@pvamu.edu; Tel.: +1(936)261-9926

Abstract: Prostate cancer is a leading cause of death among men but its genomic characterization and best therapeutic strategy are still under debate. The Genomic Fabric Paradigm (GFP) considers the transcriptome as a multi-dimensional mathematical object subjected to a dynamic set of expression correlations among the genes. Here, GFP is applied to gene expression profiles of three (one primary, and two secondary) cancer nodules and the surrounding normal tissue from a surgically removed prostate tumor. GFP was used to determine the regulation and rewiring of the P53 signaling, apoptosis, prostate cancer and several other pathways involved in survival and proliferation of the cancer cells. Genes responsible for the block of differentiation, evading apoptosis, immortality, insensitivity to anti-growth signals, proliferation, resistance to chemotherapy and sustained angiogenesis were found as differently regulated in the three cancer nodules with respect to the normal tissue. The analysis indicates that even histo-pathologically equally graded cancer nodules from the same tumor have substantially different transcriptomic organizations, raising legitimate questions about the validity of meta-analyses comparing large populations of healthy and cancer humans. The study suggests that GFP may provide a personalized alternative to the biomarkers' approach of cancer genomics.

Keywords: apoptosis; evading apoptosis; expression variability; cancer functional pathway; prostate cancer phenotype; immortality; proliferation; P53 signaling; transcriptomic network.

1. Introduction

The 28.0 02/02/2021 release of the Harmonized Cancer Datasets Genomic Data Commons Data Portal [1], that summarized 84,591 cases in 67 primary sites, identified distinct 3,461,256 cancer-related mutations in 23,535 genes (on average, 147 distinct mutations/gene). Cancer or non-cancer, 3,461,256 is close to the expected number of random mutations (~3,100,000) caused by the stochastic nature of the chemical reactions involved in the DNA replication (1/1,000 probability of a random mutation x 3,1 Gigabase pairs in the human genome). The Data Portal shows that practically every gene was found as mutated in almost all cancer forms and that every cancer forms exhibits mutations in all genes.

According to [1], 31,596 mutations in 20,202 genes (including 19,742 protein coding, 102 transcribed unprocessed pseudogenes, 67 lincRNAs, 40 IG-V genes, 37 miRNA etc) were identified so far in 2,355 cases of certified prostate cancer. The most frequently mutated genes in the prostate cancer are: *TTN* (titin, in 61 cases) and *TP53* (tumor protein p53, in 60 cases). However, mutations of these two genes are not exclusively associated to prostate cancer, being among the most 10 frequently mutated genes in many other cancer forms (adrenal gland, bladder, brain, breast, colorectal, kidney, lung, ovary, pancreas etc).

There are several commercially available cancer diagnostic assays that compare either the base sequences or the expression levels of selected genes with corresponding "standard" mutations panels (e.g. [2-6]) or "standard" transcriptomic signature of that form of cancer (e.g. [7-9]). However, there are serious doubts about what "standard"

means: is it the same for everybody, regardless of race, sex, age, tissue, environment, medical history, habits etc. of the patient or unique for each of us? Such assays were designed based on meta-analyses comparing the gene sequences or/and their expression levels in large populations of healthy and cancer individuals (e.g. [10-12]). Cancer databases compiled values reported by several research groups that used different platforms and experimental protocols, with/without considering demographically stratified populations (e.g. [13-15]).

In several papers, we proved that the gene expression profile depends on the genetic background [16], sex [17], age [18], hormones [19], disease and treatment [20, 21], and environmental conditions [22-25]. Owing to the astronomic number of possibilities, it is impossible to conceive that two individuals might have exactly the same combination of regulatory factors and also identical influences of these factors. Nevertheless, with all similarities, each human is a dynamic "unique". Therefore, a most appropriate way in cancer genomics is to refer the gene expression profile in cancer nodules to that of the surrounding cancer-free tissue of the same tumor, as became standard in many laboratories (e.g> [26-28]) including ours. Interestingly, the same cancer phenotype may exhibit distinct gene expression profiles in different individuals as we reported for two cases of metastatic prostate cancers [29]. Moreover, even in the same tumor, with the same histo-pathological grade, different cancer nodules have distinct transcriptomic organization as proved in a case of clear cell renal cell carcinoma [30] and also further in this report in a case of prostate cancer.

Several specialized software text mined the literature to select the genes and their interrelations that may have a role in the functional pathway responsible for the prostate cancer. For instance, Kyoto Encyclopedia of Genes and Genomes (KEGG, [31]) selected 97 genes involved in the prostate cancer (PRC) pathway [32]. Out of these, we quantified 84: *AKT1/2/3, AR, ARAF, ATF4, BAD, BCL2, BRAF, CASP9, CCND1/E1/32, CDK2/N1B, CHUK, CREB1/3/3L1/3L2/3L4/5/BP, CTNNB1, E2F1/2/3, EGFR, EP300, ERBB2, FGFR1/2, FOXO1, GRB2, GSK3B, GSTP1, HRAS, HSP90AA1/AB1/B1, IGF1/1R, IKBKB/GNFKBIA, NKX3-1, KLK3, KRAS, LEF1, MAP2K1/2, MAPK1/3, MDM2/9, MTOR, PDGFA/B/C/RA/RB, PDPK1, PIK3CA/B/D/R1/R2/R3, PLAT, PLAU, PTEN, RAI1, RB1, RELA, SOS1/2, SPINT1, TCF7, TCF7L1/2, TGFA, TMPRSS2, TP53, ZEB1.*

While almost all other cancer genomists limit their analyses of gene expression profiles to identifying what gene was up-/down-regulated in cancer with respect to normal tissue, we have adopted the Genomic Fabric Paradigm (GFP) [33]. GFP operates on 4-biological replicas experimental design and considers the transcriptome as a multi-dimensional mathematical object subjected to a dynamic set of expression correlations among the genes. GFP characterizes every gene in each region by: average expression level (AVE), Relative Expression Variability (REV) across biological replicas and expression correlation (COR) with each other gene from the same region and all genes from all other regions. Comparing the AVE values in two regions determines the expression ratios of the quantified genes. REV of a gene across biological replicas provides indirect estimate of the strength of the homeostatic mechanisms to control that gene transcript's abundances [29]. The expression correlation analysis is based on the "Principle of Transcriptomic Stoichiometry" [34], a generalization of the Dalton's law from chemistry, requiring the expression coordination of all genes whose encoded products a part of a functional pathway. Use of these three independent groups of features increases the workable information provided by a high throughput gene expression (microarray or RNA-sequencing) experiment by several orders of magnitude [35].

In addition to the prostate cancer pathway, GFP was used to analyze the KEGG-determined apoptosis (APO) [36], P53 signaling (P53) [37], and the (general) pathways in cancer (PAC) [38]. Within PAC, a special attention was given to the gene blocks responsible for the: evading apoptosis and immortality (EAI, 46 genes), proliferation, insensitivity to antigrowth signals and block of differentiation (PIB, 54 genes), and resistance to chemotherapy and sustained angiogenesis (RCSA, 19 genes).

 doi:10.20944/preprints202103.0242.v1

2. Results

2.1. Overview

In total, we quantified the expressions of N = 14,908 unigenes in each of the 16 quarters of the three cancer nodules (here after denoted as A, B, C) and the surrounding normal tissue (denoted by N), isolated from a surgically removed metastatic prostate tumor of a 65 y old black man. A was a primary tumor, Gleason score 4 + 5 = 9/10, while B and C were both secondary tumors with Gleason score 4 + 4 = 8/10. Raw and processed data from the four regions were deposited and are publicly accessible in the websites [39] for the N and A regions, and [40] for the B and C regions. The 4-biological replicas strategy provides for every gene in each region the values of AVE and REV. AVE was used to identify up-/down regulated genes in the A, B, C regions with respect to N and the differentially expressed genes between pairs of cancer nodule. REV analysis identified the very stably expressed genes (low REVs), critical for the survival and proliferation of each cell phenotype and the very unstably expressed genes, used by the cells as vectors of adaptation to the environmental fluctuations [41]. Moreover, quantification of tens of thousands of genes at a time from the same region provides for each gene extra 14.907 correlation coefficients (COR) with each other gene in every region and 14,908 correlations with all genes from each other region. Thus, use of GFP translated the quantified 56,632 expression values (4 regions x 14,908 genes in one region) data into 1,778,077,160 transcriptomic characteristics of the profiled tumor (119,270 times larger than the number of expression levels of the individual genes).

The smallest and the largest AVEs in the four regions were for N: bradykinin receptor B1 (*BDKRB1*; 0.11) and ribosomal protein L13 (*RPL13*; 621.27), for A: glycoprotein A33 (*GPA33*; 0.15) and *RPL13*; (288.47), for B: lymphocyte antigen 6 complex, locus G6C (*LY6G6C*; 0.07) and *RPL13* (476.68); for C: ubiquitously transcribed tetratricopeptide repeat containing, Y-linked (*UTY*; 0.09) and *RPL13* (415.06).

The most stably expressed (lowest REV) and the most unstably expressed (highest REV) genes in the four regions were for N: mitochondrial ribosomal protein S12 (*MRPS12*; 0.32%) and ubiquitously-expressed, prefoldin-like chaperone (*UXT*; 133.35%), for A: ectonucleoside triphosphate diphosphohydrolase 2 (*ENTPD2*; 0.29%) and ubiquitin specific peptidase 31 (*USP31*; 188.14%), for B: synovial sarcoma, X breakpoint 3 (*SSX3*; 0.94%) and v-maf avian musculoaponeurotic fibrosarcoma oncogene homolog K (*MAFK*; 188.56%), for C: BAI1-associated protein 2-like 1 (*BAIAP2L1;* 0.40%) and zyxin (*ZYX*; 192.35%). The median REVs are 12.79% (A), 32.39% (A), 29.73% (B) and 17.71% (C), indicating that the gene expressions are overall less controlled by the homeostatic mechanisms in the cancer regions.

The most down-regulated genes were: high mobility group AT-hook 2 (*HMGA2*; -15.88x in A), kallikrein-related peptidase 11 (*KLK11*; -57.82x in B) and peptidase inhibitor 15 (*PI15*; -30.20x in C). The most up-regulated genes were: forkhead box J1 (*FOXJ1*; 13.75x in A), phospholipase A2, group IIA (platelets, synovial fluid) (*PLA2G2A*; 18.75x in B) and scleraxis basic helix-loop-helix transcription factor (*SCX*; 300.17x in C). The exceptionally high up-regulation of *SCX* in C was a surprise given that its expression level was not altered in the other two cancer regions.

2.2. Independent characteristics of the individual genes

Figure 1 presents the visual proof that for every gene in each region, AVE, REV and COR (with each other gene from the same or other region) are independent characteristics. The independence is illustrated for the AVEs and REVs of 44 KEGG-selected evading apoptosis genes from the Pathways in cancer [37] and their correlation with *TP53* (tumor protein p53).

Preprints (www.preprints.org) | NOT PEER-REVIEWED | Posted: 9 March 2021 doi:10.20944/preprints202103.0242.v1

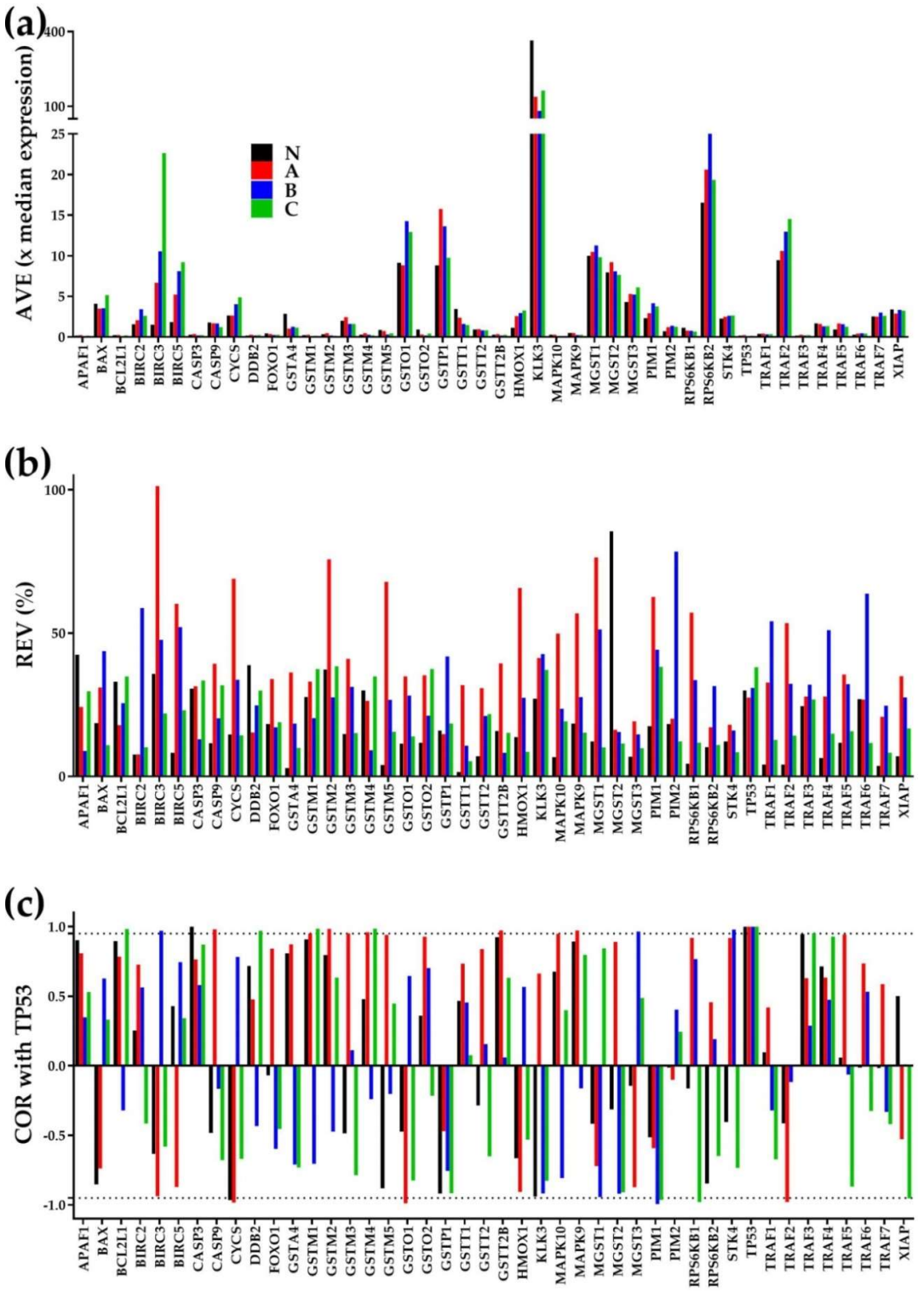

Figure 1 Three independent characteristics for every of the KEGG-determined 43 evading apoptosis genes in the three cancer nodule regions (A, B, C) and the surrounding normal tissue (N) region. (a) Average expression level (AVE) in multiples of the average expression level of the median gene. **(b)** Relative Expression Variability. **(c)** Expression correlation with *TP53*.

 doi:10.20944/preprints202103.0242.v1

In this gene selection, kallikrein-related peptidase 3 (*KLK3*) had by far the largest average expression level (measured in median gene average expression level units) in all regions (364 in N, 139 in A, 82 in B and 164 in C). *KLK3* is a prognostic marker for progression free survival in patients with metastatic prostate cancer [42].

Microsomal glutathione S-transferase 2 (*MGST2*) had the largest variability in N (REV = 86%), baculoviral IAP repeat containing 3 (*BIRC3*) had the largest variability in A (REV = 101), Pim-2 proto-oncogene, serine/threonine kinase (*PIM2*) in B (REV = 79%) and glutathione S-transferase mu 2 (*GSTM2*) in C (REV = 39%). *MGST2* was recently reported as critical in aristolochic acid-induced gastric tumor process [43]. *BIRC3* [44] and *PIM2* [45] are recognized anti-apoptotic factors, and *GSTM2* is a biomarker for the early stages of the prostate cancer [46].

COR analysis, validated by the unit values of the correlation of *TP53* with itself in all four regions, indicates also different levels of synergism/antagonisms both across the regions for the same gene and across the genes within the same region. Expression correlations of two genes can be also opposite in different regions, indicating that the encoded products of the two genes act synergistically in one region and antagonistically in the other. For instance, BIRC3 has a ($p < 0.05$) significant antagonism with TP53 in A but a significant synergism in B (and a not significant antagonism in C.

Figure 1 shows also the substantial differences among the three cancer nodules with respect to each of the three independent variables.

2.3. Three ways to measure the expression regulation

Figure 2 presents the regulation of the KEGG-determined 44 evading apoptosis genes in the three cancer nodule regions (A, B, C regions) with respect to the surrounding normal tissue (N region). The regulation is shown as: (a) uniform (+1/-1) contribution to the percentages of up-/down-regulated genes, (b) expression ratio "x" and (c) Weighted Individual (gene) Regulation (WIR). Both x and WIR are negative for down-regulated genes. While (a) is limited to only significantly regulated genes based on arbitrary cut-off criteria for the absolute fold-change and the p-value of the heteroscedastic *t*-test of the means' equality, (b) and (c) considers all genes and discriminate their contributions. For instance, although the up-regulation of *BIRC3* had the same contribution to the percentage of up-regulated genes in both B and C compared to N, the expression ratio in C (x = 14.89) is statistically significantly larger than in B (x = 6.94) and so is the WIR (21.05 in C and 8.71 in B). However, although in this gene selection, the expression ratio with respect to N was the largest for *BIRC3* in C, it is the down-regulation of *KLK3* that had the largest contribution (WIR = - 585.50 in A, -1,248.43 in B and – 439.17 in C) to the transcriptomic alteration in all cancer nodules B, owing to its large expression level in the reference tissue (region N).

Preprints (www.preprints.org) | NOT PEER-REVIEWED | Posted: 9 March 2021 doi:10.20944/preprints202103.0242.v1

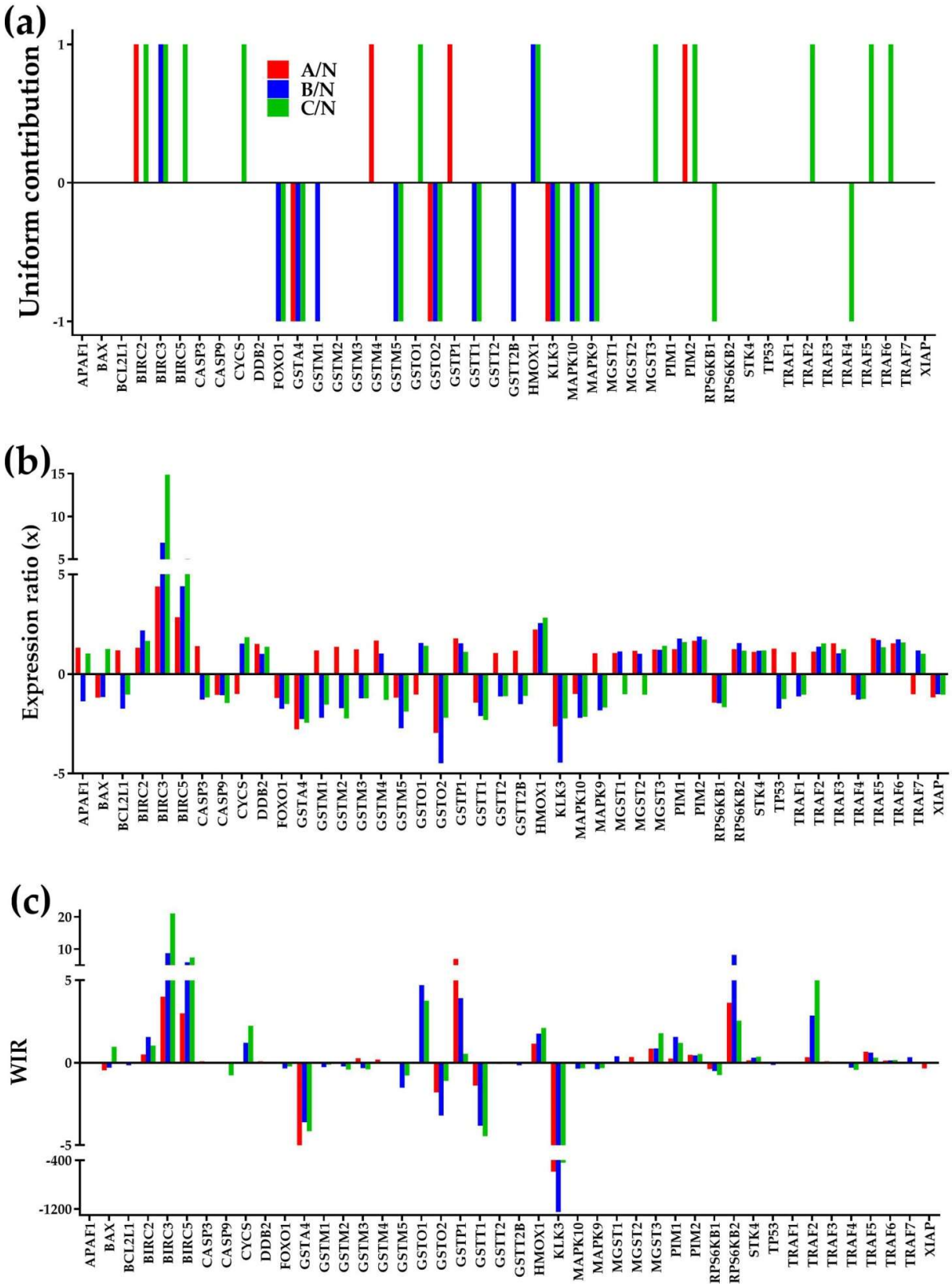

Figure 2 Regulation of the 44 evading apoptosis genes in the three cancer nodules (A, B, C) with respect to the normal tissue (N) measured as (a) uniform contribution, (b) expression ratio "x" and (c) Weighted Individual (gene) Regulation "WIR".

 doi:10.20944/preprints202103.0242.v1

2.4. Regulation of selected functional pathways in the cancer nodules with respect to the normal tissue

Figure 3 presents the regulation of the major KEGG-determined functional pathways: APO (117 quantified genes), P53 (62 genes), PRC (84) and selected component blocks from the pathways in cancer PCA (119 from a total of 530 genes). The selected blocks were: EAI (46 genes), PIB (54 genes), RCSA (19 genes). The pathway regulations were quantified as percentages of up- and down-regulated genes and as Weighted Pathway Regulation (WPR). For comparison, we added also the numbers when all (ALL) 14,908 quantified genes are considered. Of note is that nodule B had the significantly largest WPRs for the EAI, PIB and PRC groups of genes, while nodule C had the significantly largest percentages of up-regulated genes in all pathways. Of note is also the finding that in all cancer nodules more genes related to cancer cell survival and proliferation are up- than down-regulated, while more genes involved in apoptosis and P53 signaling are down-regulated than up-regulated.

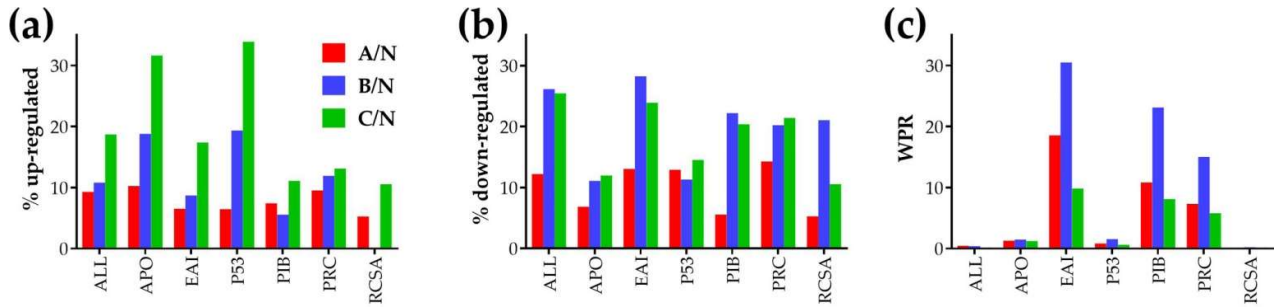

Figure 3 Overall regulation of selected KEGG-determined functional pathways measured by the percentages of the significantly down- (a) and up-regulated (b) genes, and by the Weighted Pathway Regulation (WPR) (c). ALL = all genes, APO = apoptosis, EAI = evading apoptosis + immortality, P53 = P53 signaling, PIB = proliferation + insensitivity to antigrowth signals + block of differentiation, PRC = prostate cancer, RCSA = resistance to chemotherapy and sustained angiogenesis.

2.5. Differential regulation of the genes central to the KEGG-determined prostate cancer pathway in the three cancer nodules

Figure 4 shows the regulation of individual genes at the center of the KEGG-determined prostate cancer pathway [32], blocks of genes presented in panel **(a)**. Although not very abundant, there are still differences in the subsets of regulated genes among the three nodules. The up-regulation of *MMP9* (matrix metallopeptidase 9 (gelatinase B) is in line with the reported higher expression in the serum of patients with lung [47] and prostate [48] cancer. Although *AKT2* (v-akt murine thymoma viral oncogene homolog 2) was down-regulated in all three cancer nodules (x = -1.65 in A, - 1.61 in B and -1.94 in C), *AR* (androgen receptor) was not affected and therefore the tumor did not regress as expected in androgen deprivation therapy [49].

 doi:10.20944/preprints202103.0242.v1

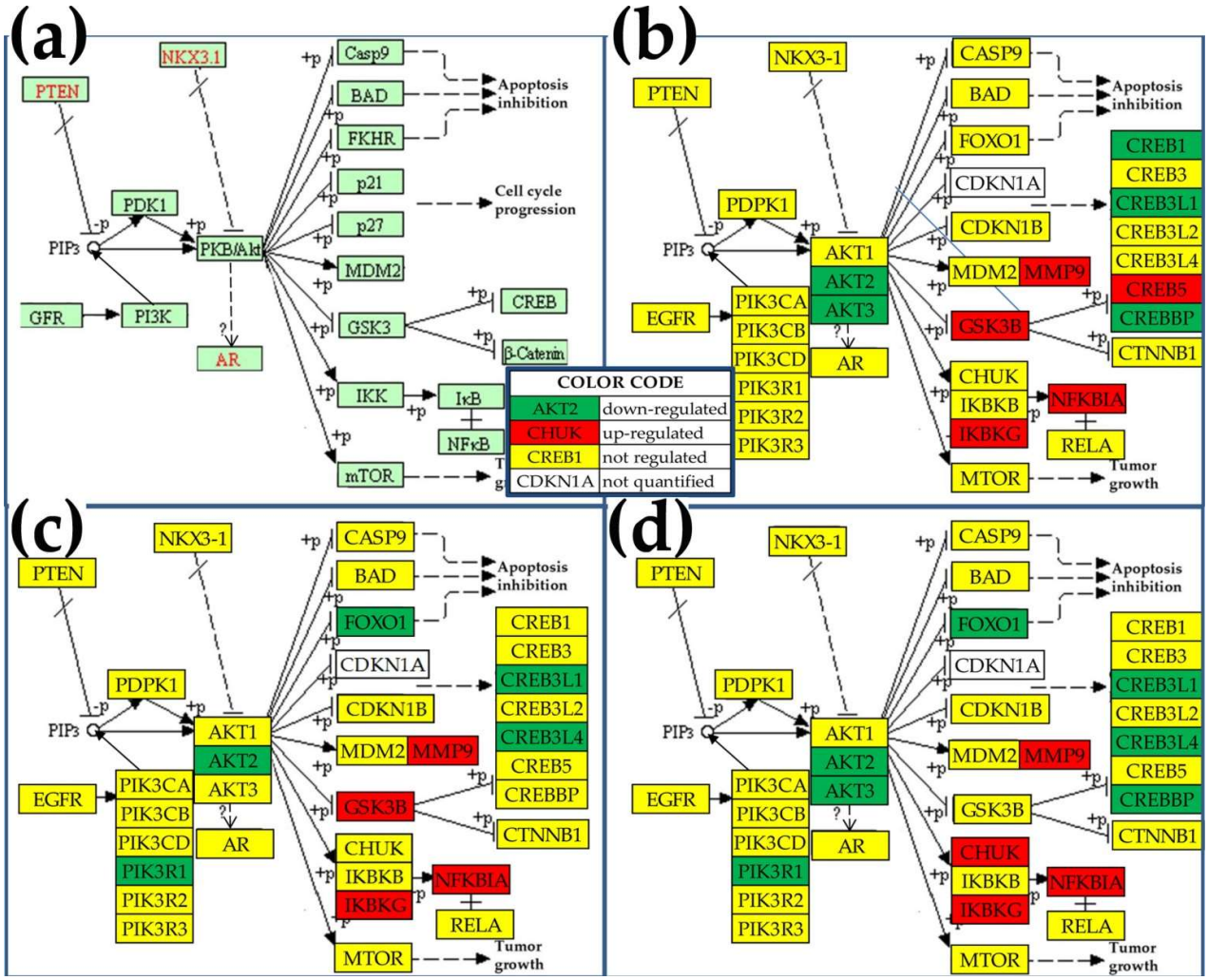

Figure 4 Significantly regulated genes central to the KEGG-determined prostate cancer functional pathway (a) in the nodule A (b), nodule B (c) and nodule C (d) with respect to the surrounding normal tissue. Regulated genes: *AKT2/3* (v-akt murine thymoma viral oncogene homolog 2/3), *CREB1/5* (cAMP responsive element binding protein 1/5), *CREB3L1/4* (cAMP responsive element binding protein 3-like 1/4), *CREBBP* (CREB binding protein), *FOXO1* (forkhead box O1), *GSK3B* (glycogen synthase kinase 3 beta), *IKBKG* (inhibitor of kappa light polypeptide gene enhancer in B-cells, kinase gamma), *MMP9* (matrix metallopeptidase 9 (gelatinase B)), *NFKBIA* (nuclear factor of kappa light polypeptide gene enhancer in B-cells inhibitor, alpha), *PIK3R1* (phosphoinositide-3-kinase, regulatory subunit 1 (alpha)). (modified from [9])

2.6. Regulation of individual genes responsible for survival and proliferation of cancer cells

Figures 5a, 5b and 5c present the expression regulation of genes identified by KEGG [38] as linked in most cancer forms to the: block of differentiation, evading apoptosis, immortality, insensitivity to anti-growth signals, proliferation, resistance to chemotherapy and sustained angiogenesis. Genes such are: *GSTA4, GSTO2, KLK3, PGF* were down-regulated and *E2F2, MMP9, PIM2, VEGFC* are up-regulated in all cancer nodules. Other genes were regulated only in one nodule, e.g.: *CSF1R, CYCS, E2F3, GSTM1,*

GSTM4, *GSTO1*, *GSTP1*, *GSTT2B*, *HES1*, *HEY1*, *HEYL*, *HHIP*, *MGST3*, *MYC*, *RARA*,... There are also genes regulated similarly in two nodules: *BIRC2*, *BIRC3*, *BMP4*, *CCNA2*, *CCND1*, *E2F1*, *FOXO1*, *GLI1*, *GSTM5*, *GSTT1*, …. However, no gene was found as oppositely regulated in two cancer nodules.

Of note are the differences in the subsets of significantly regulated genes among the three cancer nodules.

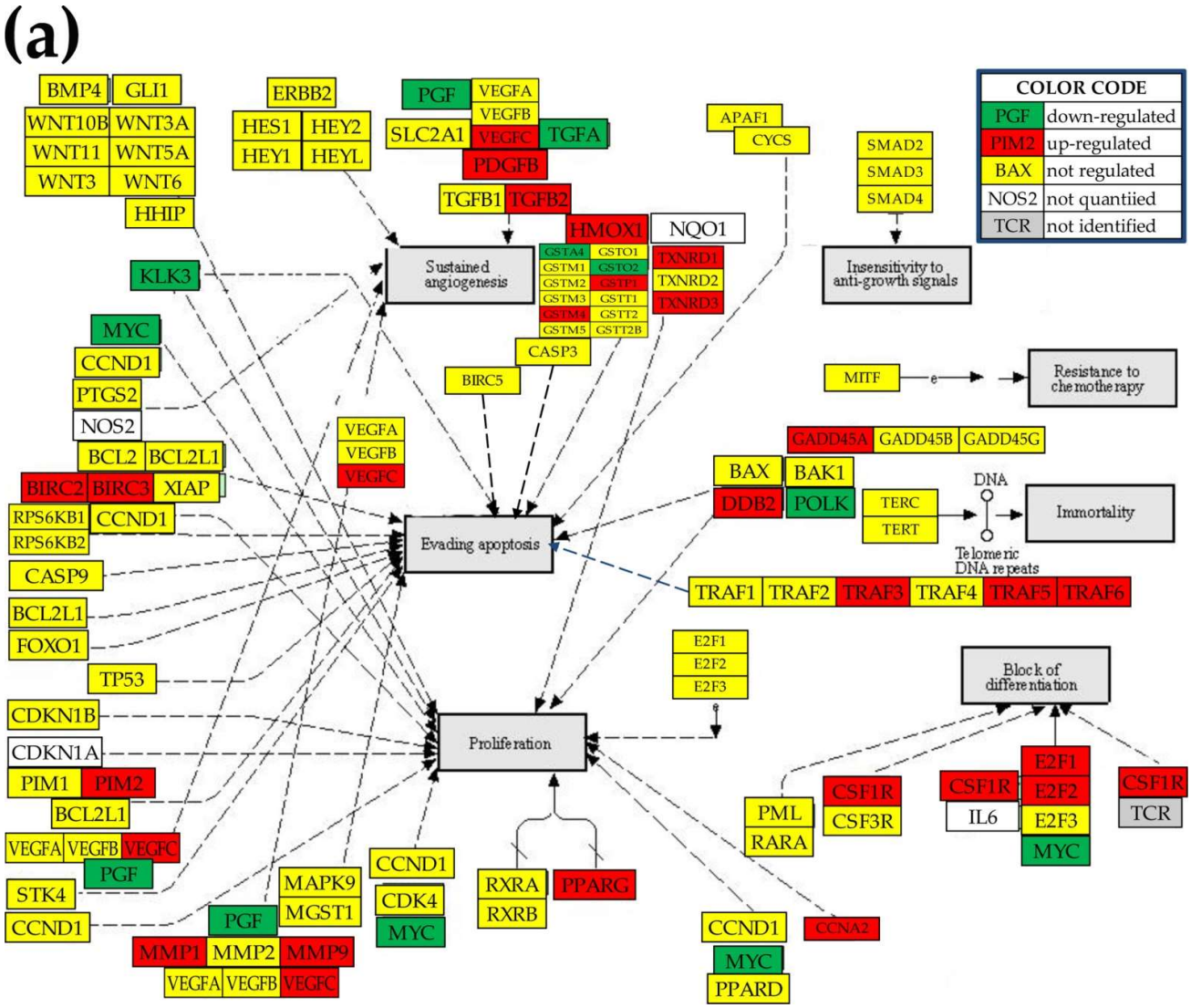

 doi:10.20944/preprints202103.0242.v1

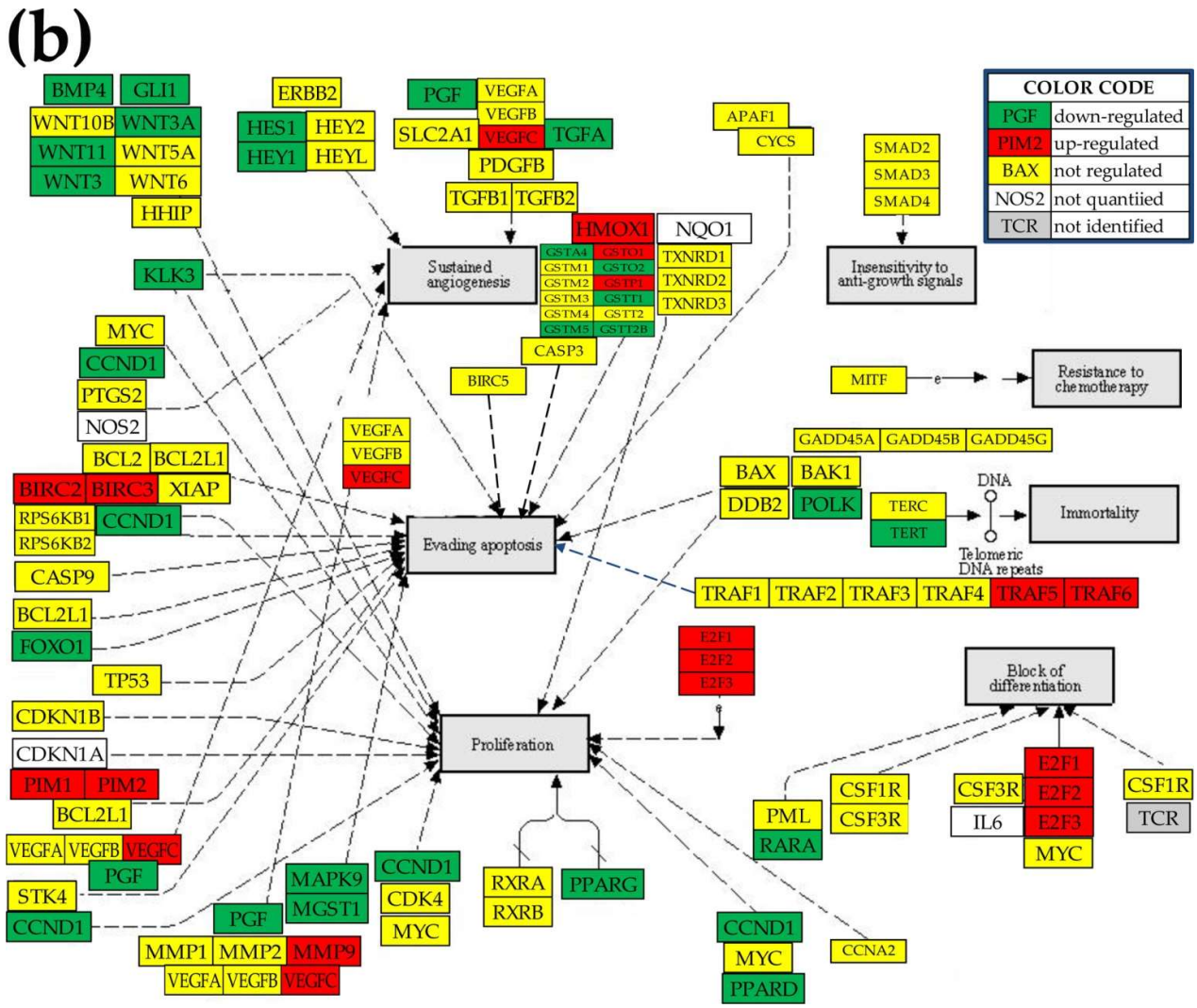

 doi:10.20944/preprints202103.0242.v1

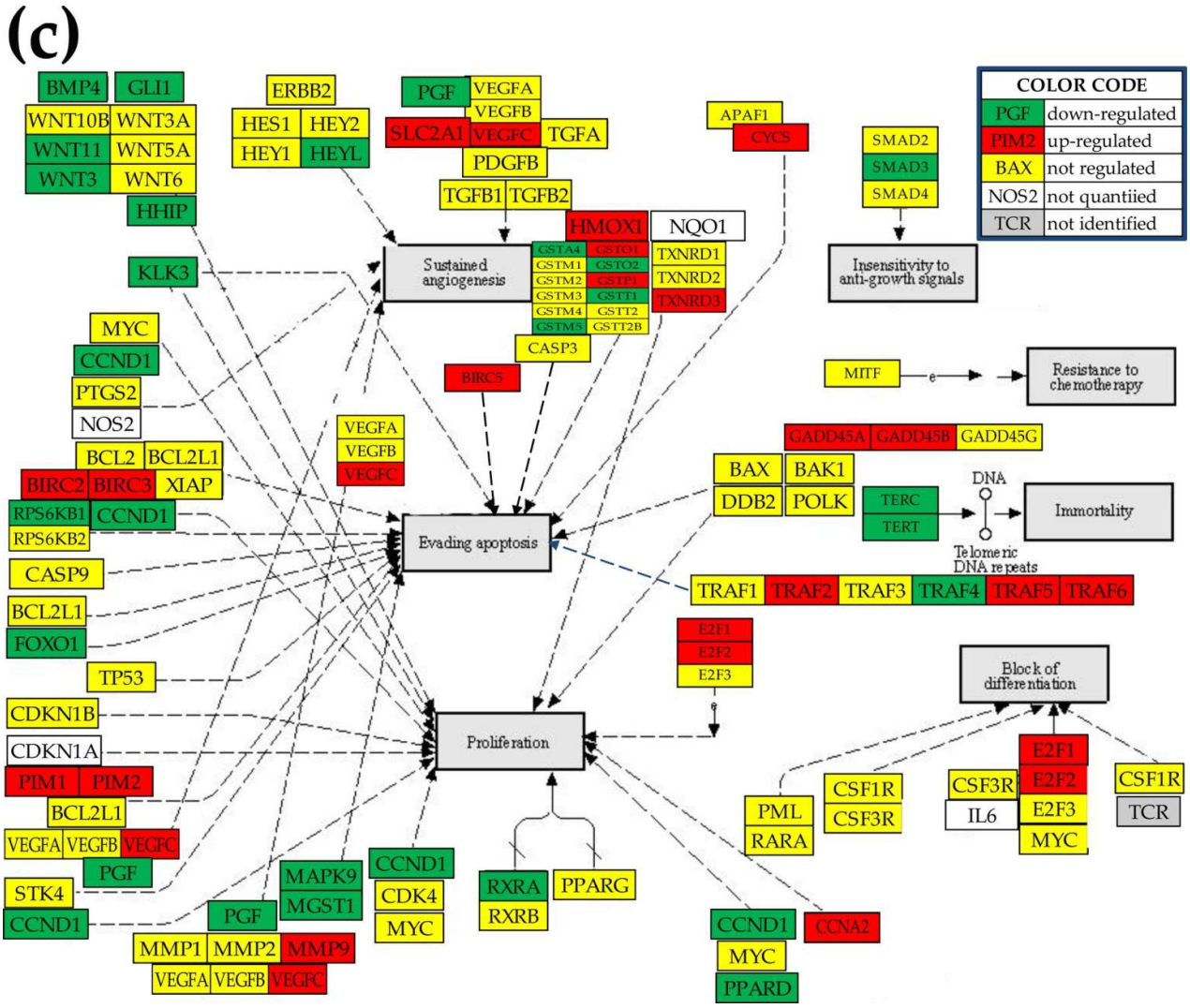

Figure 5 Regulation of genes identified by KEGG as associated to cancer cell survival and proliferation. (**a**) Nodule A; (**b**) Nodule B; **(c)** Nodule C. Regulated genes: *BIRC2/3/5* (baculoviral IAP repeat containing 2/3/5), *BMP4* (bone morphogenetic protein 4), *CCNA2/D1* (cyclin A2/D1), *CSFIR* (colony stimulating factor 1 receptor), *DDB2* (damage-specific DNA binding protein 2, 48kDa), *E2F1/2/3* (E2F transcription factor 1/2/3), *FOXO1* (forkhead box O1), *GLI1* (GLI family zinc finger 1), *GSTA4/M1/M4/M5/O1/O2/P1/T1/T2B* (glutathione S-transferase alpha 4/mu 1/mu 4/mu 5/omega 1/omega 2/pi 1/theta1/theta 2B), *HES1* (hes family bHLH transcription factor 1), *HEY1/L* (hes-related family bHLH transcription factor with YRPW motif 1/like), *HHIP* (hedgehog interacting protein), *HMOX1* (heme oxygenase (decycling) 1), *KLK3* (kallikrein-related peptidase 3), *MAPK9/10* (mitogen-activated protein kinase 9/10), *MGST3* (microsomal glutathione S-transferase 3), *MMP1/9* (mitogen-activated protein kinase 1/9), *MYC* (v-myc avian myelocytomatosis viral oncogene homolog), *PGF* (placental growth factor), *PIM2* (Pim-2 proto-oncogene, serine/threonine kinase), *RARA* (retinoic acid receptor, alpha), *RPS6KB1* (ribosomal protein S6 kinase, 70kDa, polypeptide 1), *RXRA* (retinoid X receptor, alpha), *SLC2A1* (solute carrier family 2 (facilitated glucose transporter), member 1), *SMAD3* (SMAD family member 3), *TERC* (telomerase RNA compo-

 doi:10.20944/preprints202103.0242.v1

nent), *TERT* (telomerase reverse transcriptase), *TGFA/B2* (transforming growth factor, alpha/BETA 2), *TRAF4/5/6* (TNF receptor-associated factor 4/5/6), *TXNRD3* (thioredoxin reductase 3), *VEGFC* (vascular endothelial growth factor C), *WNT3/11/3A* (wingless-type MMTV integration site family, member 3/11/3A).

2.7. *Remodeling of the prostate cancer transcriptomic networks*

Figure 6 presents the statistically ($p < 0.05$) significant expression synergism, antagonism and independence of the first alphabetically ordered 25 KEGG-identified prostate cancer-related genes in the normal tissue and each of the cancer nodules. One may observe that each cancer nodule had higher expression (synergistic + antagonistic) coordination and lower independence than the normal tissue, indicating stronger intercoordination of the prostate cancer genes in the cancer nodules. Thus, 12.02% total coordination in A > 9.04% total coordination in C > 8.38% total coordination in B > 6.13% total coordination in N. Of note are also the coordination differences among the three cancer nodules.

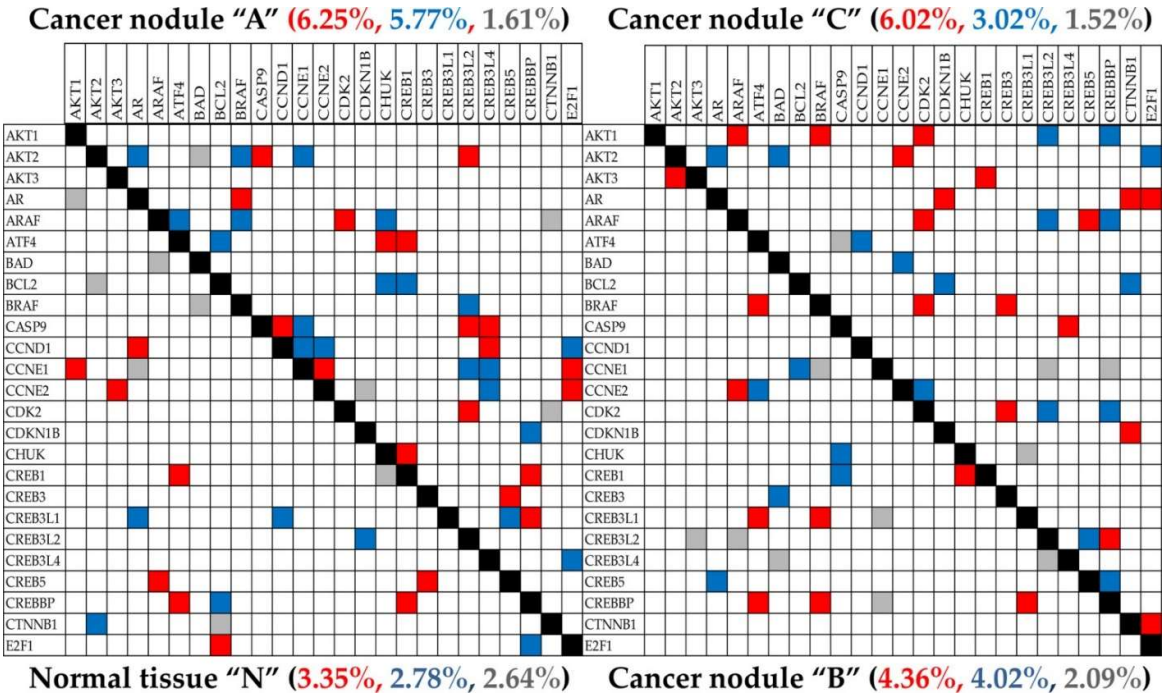

Figure 6 Statistically ($p < 0.05$) significant expression synergism, antagonism and independence of the first 25 alphabetically ordered KEGG-identified prostate cancer-related genes in the normal tissue (N) and each of the three cancer nodules (A, B, C). Red/blue/gray squares indicate significant expression synergism/anatgonism/ independence of the genes labeling the intersecting raws and columns in that profiled region. Red/blue/gray numbers are the percentages of significant expression synergism/ anatgonism/independence among all 84 prostate cancer genes quantified in that region. Owing to the correlation analysis symmetry to the permutation of the correlated genes, only the below or over the diagonal (black squares) part of the diagram was shown for each condition.

2.7. Alteration of the TP53 targeted genes network in prostate cancer

Figure 7 presents the network of TP53 targeted genes in the four profiled region.

Preprints (www.preprints.org) | NOT PEER-REVIEWED | Posted: 9 March 2021 doi:10.20944/preprints202103.0242.v1

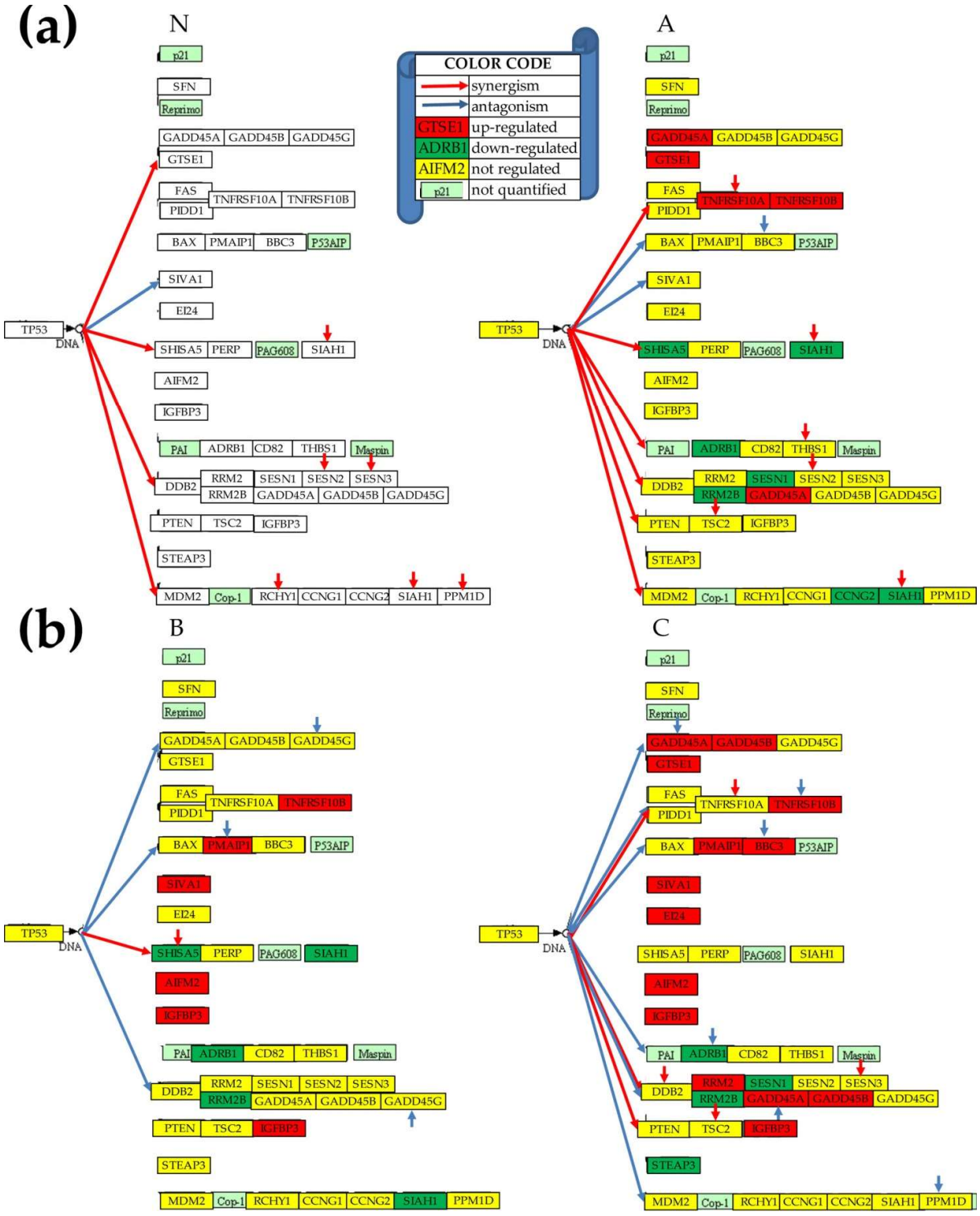

Figure 7 Expression coordination of *TP53* with KEGG-determined targeted genes in (a) normal tissue; **(b) cancer nudule A; (c)** cancer nodule B; **(d)** cancer nodule C. Little arrows indicate the significantly coordinated genes within the corresponding group of genes. Red/green/yellow background of a gene symbol in a cancer region indicates whether that gene was up-/down- or not significantly regulated in the represented cancer region with respect to the normal tissue. Quantified genes in N have the symbols in white

background. Light green background of a block indicates that no gene was quantified in that block.

According to KEGG [37], all these blocks of genes should be activated by *TP53*, meaning that when expression of *TP53* goes up expression of the activated genes should go up too (i.e. synergistic expression). However, only part of the targeted genes were actually synergistically expressed with *TP53* in the normal prostate tissue (*GTSE1, SIAH1 SESN2, SESN3 RCHY1, PPMID*) and one (*SIVA1*) was antagonisticaly expressed. The expression correlations in the normal tissue were substantially (but differently) altered in the three cancer nodules. The numbers of correlations ranged from 1 synergism and 3 antagonisms in B to 5 synergisms and 2 antagonisms in A, and 4 synergisms and 5 antagonisms in C. The subsets of significantly regulated genes were also different in the three cancer nodules: 4 up- and 6 down-regulated in A, 5 up- and 3 down-regulated in B, and 13 up- and 4 down-regulated in C.

2.8. In-phase and in anti-phase expression of prostate cancer genes among the three cancer nodules

Figure 8 presents the KEGG-identified prostate cancer genes that are statistically ($p < 0.05$) significantly expressed in-phase and in anti-phase between all pairs of profiled regions of the tumor. This analysis is based on our model of transcellular transcriptomic networks [50] that we have also applied to identify syncronous expression of ion channels between adjacent heart chambers [51].

One may note that the cancer nodules have different in-phase and in anti-phase expression both among themselves and with the normal tissue region, regions A and B having the largest in-phase expressions. Interestingly, while region C has the least in-phase and in anti-phase expressions with both regions A and B, it has the highest number of in-phase expressions with the normal tissue. We found that *ERBB2* (a.k.a. *HER2*) is expressed in-antiphase in N with respect to nodules A and B but in-phase in these two nodules. This finding justifies the reports that *ERBB2* activation is associated with tumor-intiating cells contribution and progression of prostate cancer [52].

Preprints (www.preprints.org) | NOT PEER-REVIEWED | Posted: 9 March 2021 doi:10.20944/preprints202103.0242.v1

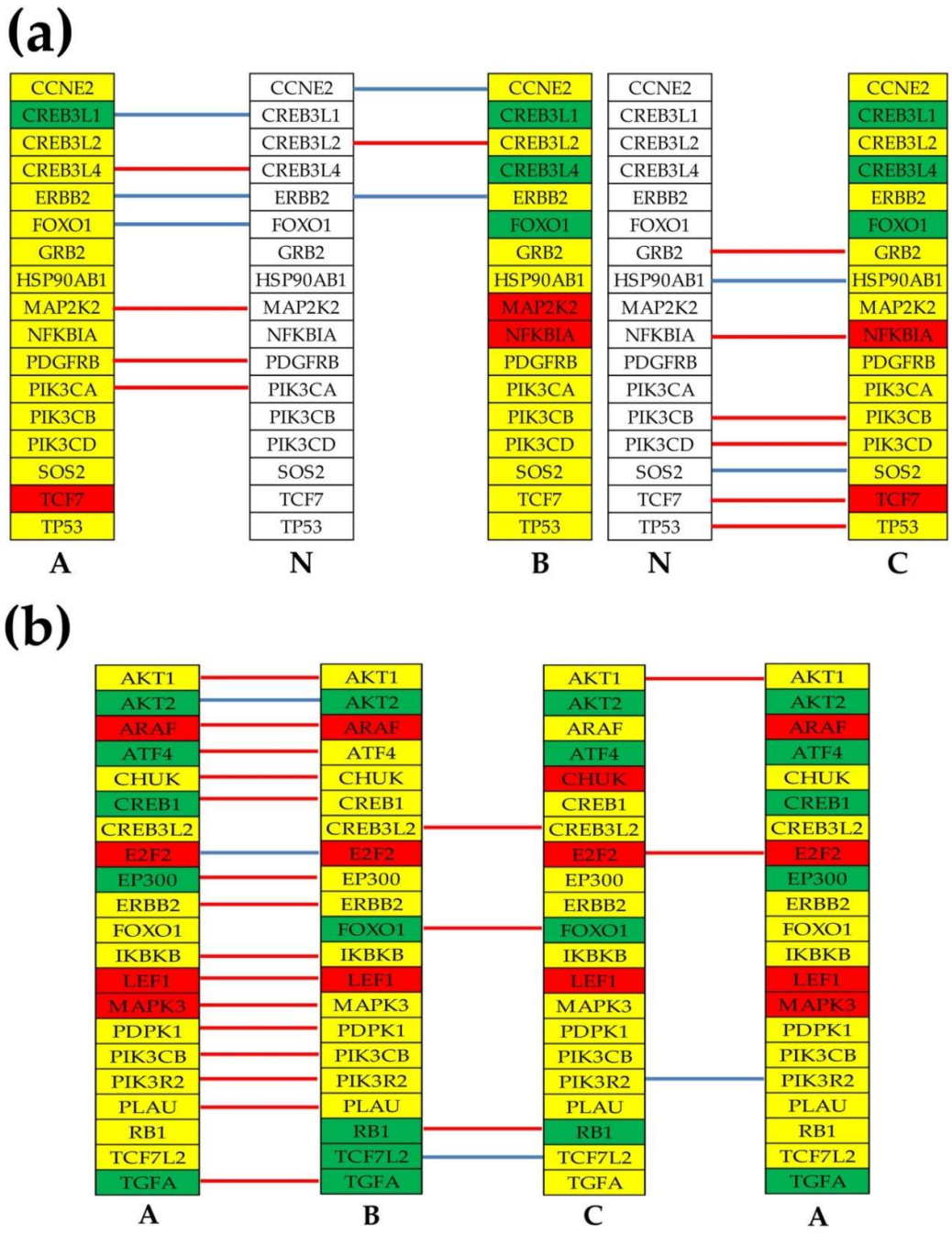

Figure 8 Statistically ($p < 0.05$) significantly in-phase (synchronously) and in-antiphase expressed KEGG-determined prostate cancer genes in pairs of regions. **(a)** Synchrony and anti synchrony of normal tissue paired with each cancer nodule. **(b)** Synchrony and anti synchrony among cancer nodules. Red/green/yellow background of a gene symbol in a cancer region indicates whether that gene was up-/down- or not significantly regulated in the represented cancer region with respect to the normal tissue. Quantified genes in N have the symbols in white background.

 doi:10.20944/preprints202103.0242.v1

3. Discussion

In this study, we analyzed the gene expression profiles of three cancer nodules and the surrounding normal tissue from the same surgically removed prostate tumor. Our analyses indicated that although B and C of the three cancer nodules were equally graded (Gleason score: 4 + 4 = 8/10) from histopathological point of view, their transcriptomes were different. The differences among the three cancer nodules were evident in all analyses; however the most intriguing were those between the phenotypically similar regions B and C.

These results prove again the existence of transcriptomic redundancy (many distinct transcriptomes) of each cancer phenotype. We have arrived at the same conclusion not only for different persons (equally graded cases of prostate cancer [29]), but even for equally graded cancer nodules from the same tumor (one case of clear cell renal cell carcinoma [30]).

The Genomic Fabric Paradigm [53] approach provided the most theoretically possible comprehensive understanding of the topologies of the transcriptomes of the four regions and their interplays. GFP characterized each profiled region by three independent groups of variables: average expression levels (AVEs), relative expression variabilities (REVs) and expression correlations (CORs) of all gene pairs. We proved their independence in Figure 1 (p-val $<10^{-200}$) for each comparison between the sets of any two characteristics of all genes in a region). Moreover, GFP explores also the transregional transcriptomic networks by identifying what genes are expressed in-phase (synchrony) or in anti-phase in the corresponding regions.

The largest expression of the ribosomal protein *RPL13* in all four regions (621.27 in N, 288.47 in A, 476.68 in B and 415.06 in C) did not come as a surprise since more than half of the 50 most largely expressed genes in each region encode ribosomal proteins: 26 in N, 31 in A, 37 in B and 33 in C. Surprisingly, more ribosomal genes were down-regulated than up-regulated in each cancer nodule, although their preferred down-regulation was somehow compensated by the preferred up-regulation of polymerase subunits and translation initiation factors.

REV analysis determined the regions' overall hierarchy with regard to the median expression variability: A (32.39%) > B (29.73%) > C (17.71%) > N (12.79%). Since in thermodynamics, systems closer to equilibrium exhibit higher numbers of degrees of freedom (and by consequence larger variability), we speculate that these results justifies why the cancer nodules are more robust systems (particularly the primary tumor A), with higher survival and proliferation rates.

REV analysis pointed also to some interesting genes for oncogenomics. Thus, *MRPS12*, the most stably expressed gene in N, is a potential prognostic candidate for the ovarian cancer [54], while *UXT* the most unstably expressed gene in N is associated with advanced stages of the gastric cancer [55]. *ENTPD2*, the most stably expressed gene in A is a biomarker for lung [56] and hepatocellular [57] carcinomas, while *USP31*, the most variably expressed gene in A, could be a potential target for sarcomas [58]. *SSX3*, the most stably expressed in B is a prognostic predictor for pancreatic ductal adenocarcinoma [59], while *MAFK*, the most variably expressed gene in B, appears responsible for induction of breast cancer [60]. *BAIAP2L1*, the most stably expressed gene in C, is overexpressed in clear cell renal cell carcinoma [61] as we also found in all tree prostate cancer nodules, while *ZYX*, the most variably expressed gene in C and a crucial mechanotransductor in prostate cancer [62], had also a very large (176.65x) up regulation in C. (*ZYX* was also up-regulated in A by 2.53x and B by 2.92x). The significant difference in the fold-change of this gene between nodules B and C suggests distinct mechanotransduction mechanisms (worth to be further investigated by molecular and physiological studies). The median REVs are 12.79% (A), 32.39% (A), 29.73% (B) and 17.71% (C), indicating that the gene expressions are overall less controlled by the homeostatic mechanisms in the cancer regions.

Interestingly, *HMGA2*, the strongest down-regulated gene in A (-15.88x), "whose silencing promotes apoptosis and inhibits migration and invasion of prostate cancer cells" [63], was not regulated in B and C. With *KLK11* down-regulated by -7.37x in A, -57.82x in B and -27.11x, our study confirmed previous reports [e.g. 64] of the down-regulation in cancer regions with respect to the surrounding benign tissue in prostate tumors. The observed up-regulation in all three cancer nodules of *FOXJ1* (13.75x in A, 18.51 in B and 20.39 in C) and *PLA2G2A* (6.68x in A, 18.75x in B and 23.61x in C) confirmed findings of other authors [65, 66].

Much more comprehensive than the fold-change, WIR analysis identified the genes with the largest contributions the cancer-related transcriptomic alterations. Thus, the main contributors in A were: zinc finger protein 865 (*ZNF865*) and immunoglobulin lambda-like polypeptide 5 (*IGLL5*), in B: spondin 2, extracellular matrix protein (*SPON2*) and *IGLL5*, while in C they were: *SPON2* and midkine (neurite growth-promoting factor 2) (*MDK*). *IGLL5*, the main positive contributor to both nodules A and B, was correlated with tumor-infiltrating immune cells in kidney cancer [67], suggesting an interesting study to determine whether it plays a similar role in the prostate cancer. *SPON2* is considered a more prostate-cancer specific diagnostic biomarker [68]. *MDK* is considered one as the most prognostic for short prostate cancer-specific survival [69]. For now, we have no info about the potential roles of *ZNF865* in the progression of the prostate cancer.

In Figures 3, 4 and 5 one may observe the differences among the subsets of significantly regulated genes in the three cancer regions.

As illustrated in Figures 1(c) and 6, in addition to the expression level and expression variability, cancer remodels also the transcriptomic networks by which genes are linked to each-other in functional pathways. Importantly, the remodeling was different from one cancer region to the other. These findings prove that the KEGG-designed functional pathways are not universally wired but are dependent on the cell phenotype. As such, the same manipulation of the expression of one gene may have different ripple consequences on the other genes of the pathway in distinct phenotypes. (We arrived at the same conclusion when conditionally knocking down *Gja1* gene encoding the gap junction channel protein Cx43 in the brains of two mouse strains [16]). By consequence, an efficient gene therapy for one person may not be as efficient for another person. Moreover, the treatment efficiency may be even different for distinct cancer nodules from the same tumor.

Figure 7 brings another confirmation of the transcriptomic networks' dependence not only on the cell phenotype (compare regions N and A), but also on the location of the same phenotype within the tumor (compare B and C). We found that *TP53* activation of the target genes is substantially different among the four profiled regions of the tumor. The negative correlation of *TP53* and *SIVA1* in both normal tissue and the primary tumor A (Figure 7a), suggests that increased expression of *SIVA1*, reported to inhibit cervical cancer progression [70] (and hopefully also the progression of prostate cancer) may be achieved by down-regulating *TP53*. This possibility is based on our "see-saw" model [71]. However, the correlation of *TP53* with *SIVA1* is poor in the other two cancer nodules, indicating that down-regulating *TP53* may have no consequences for *SIVA1* in the secondary tumors.

Lastly, we analyzed whether there is transcriptomic communication among the profiled regions by determining the expression correlation of KEGG-determined prostate cancer genes between two regions. A positive correlation means that the expression of that gene goes up and down simultaneously (in-phase) in both regions, while a negative correlation means that when the expression of one gene goes up in one region it goes down in the other (in-antiphase). In previous studies ([50, 51]) we have provided experimental evidence about transcellular transcriptomic communication between astrocytes and oligodendrocytes in the brain and between the myocardial walls of the adjacent heart chambers of the mouse. This type of analysis may provide clues about the transcriptomic integration of heterogeneous tissues.

4. Materials and Methods

4.1. Prostate tissues

We used the data obtained by profiling the primary tumor (hereafter denoted as region A), two secondary tumors (denoted as regions B and C), and the surrounding cancer-free tissue (denoted by N) from a surgically removed prostate of a 65y old black man. The primary tumor had the Gleason score 4 + 5 = 9/10 and the two secondary tumors had both the same Gleason score 4 + 4 = 8/10.

Each of the 6–8 mm samples collected from the four regions was split into four parts and each quarter profiled separately. Although the selected regions were as homogeneous as possible, cells of different phenotypes were not completely eliminated, and by consequence, expression of genes from other cell phenotypes affected (diluted) the reported results.

4.2. Microarray

At the time, we had equal access to Illumina NextSeq 500 but we preferred to use Agilent 4x44k human dual-color microarrays (configuration G2519F, platform GPL13497 [72]) for their excellent reliability and affordable price. We used our standard protocol [73] for the RNA extraction with RNAEasy Minikit (Qiagen, Germantown, MD, USA), purification and quantification before and after reverse transcription in the presence of Cy3/Cy5 dUTP with a Thermo Fisher Scientific NanoDrop ND-1000 (Waltham, MA, USA). RNA quality was checked with a 2100 Bioanalyzer (Santa Clara, CA, USA). 825 ng of differently (Cy3/Cy5) labeled biological replicas of the same prostate region were hybridized 17 h at 65 °C with microarrays and the washed and dried chips were scanned with an Agilent G2539 dual laser scanned for 20 bit at 5μm resolution. The digital images (tiffs) were primarily analyzed with (Agilent) Feature Extraction vs. 11.6 software. The spots with saturated or corrupted pixels, and those with the fluorescence foreground less than twice the fluorescence background were eliminated from the analysis. We used our iterative procedure alternating intra-array and inter-arrays adjustment to normalize the raw data to the median gene expression [74].

4.3. Transcriptomic analyses

The separately profiled four quarters of tumor samples from each prostate tumor region were considered as the same system subjected to four slightly different (not regulatory) environmental conditions. Thus, the expression variability of the quantified genes among these biological replicas provided indirect estimate of how much their transcripts' abundances are controlled by the cellular homeostatic mechanisms.

Because the Agilent microarrays probe some genes redundantly with several (not uniform numbers of) spots, the independent characteristics of every gene across biological replicas: average expression level (AVE), Relative Expression Variability (REV) and correlation (COR) with expression of other genes were determined using the expression levels of all valid spots as:

$$AVE_i^{(region)} = \frac{1}{R_i}\sum_{k=1}^{R_i}\mu_{i,k}^{(region)} = \frac{1}{R_i}\sum_{k=1}^{R_i}\left(\frac{1}{4}\sum_{j=1}^{4}a_{i,k,j}^{(region)}\right) \quad , \quad where:$$

$region = N, A, B, C$

$R_i =$ number of spots probing redundantly gene "i",

$a_{i,k,j}^{(region)}$ = expression level of gene "i" probed by spot "k" on biological replica "j" in "region"

$$REV_i^{(region)} = \underbrace{\frac{1}{2}\left(\sqrt{\frac{r_i}{\chi^2(r_i;0.975)}} + \sqrt{\frac{r_i}{\chi^2(r_i;0.025)}}\right)}_{\text{correction coefficient}} \underbrace{\sqrt{\frac{1}{R_i}\sum_{k=1}^{R_i}\left(\frac{s_{ik}^{(region)}}{\mu_{ik}^{(region)}}\right)^2}}_{\text{pooled CV}} \times 100\%$$

μ_{ik} = average expression level of gene i probed by spot k (= 1, ..., R_i) in the 4 biological replicas

s_{ik} = standard deviation of the expression level of gene i probed by spot k

$r_i = 4R_i - 1 =$ number of degrees of freedom

$$COR_{ig}^{(region)} = \frac{\sum_{k_i=1}^{R_i}\sum_{k_g=1}^{Rg}\left(\sum_{j=1}^{4}\left(a_{i,k,j}^{(region)} - AVE_i^{(region)}\right)\left(a_{g,k,j}^{(region)} - AVE_g^{(region)}\right)\right)}{\sqrt{\sum_{k_i=1}^{R_i}\left(\sum_{j=1}^{4}\left(a_{i,k,j}^{(region)} - AVE_i^{(region)}\right)^2\right)\sum_{k_g=1}^{R_g}\left(\sum_{j=1}^{4}\left(a_{g,k,j}^{(region)} - AVE_g^{(region)}\right)^2\right)}} \quad , \quad where \text{ "}g\text{" is another gene}$$

A gene was considered as statistically ($p < 0.05$) significantly regulated in a cancer nodule ("cancer") with respect to the normal tissue if the absolute fold-change x and the p-value ($p_i^{(N\to cancer)}$) of the heteroscedastic t-test of the means equality in the two regions satisfy the composite criterion:

$$\left|x_i^{(N\to cancer)}\right| > CUT_i^{(N\to cancer)} = 1 + \frac{1}{100}\sqrt{2\left(\left(REV_i^{(N)}\right)^2 + \left(REV_i^{(cancer)}\right)^2\right)} \quad \wedge \quad p_i^{(N\to cancer)} < 0.05$$

$where: cancer = A, B, C$

$$x_i^{(N\to cancer)} \equiv \begin{cases} \dfrac{\mu_i^{(cancer)}}{\mu_i^{(N)}} & , \text{ if } \mu_i^{(cancer)} > \mu_i^{(N)} \\ -\dfrac{\mu_i^{(N)}}{\mu_i^{(cancer)}} & , \text{ if } \mu_i^{(cancer)} < \mu_i^{(N)} \end{cases} \quad , \quad \mu_i^{(N/cancer)} = \frac{1}{R_i}\sum_{k=1}^{R_i}\mu_{ik}^{(N/cancer)}$$

As the most comprehensive measure of expression alteration, we computed also the Weighted Individual (gene) Regulation (WIR) and, for an entire functional pathway Γ, the Weighted Pathway Regulation (WPR) as:

$$WIR_i^{(N\to cancer)} = AVE_i^{(N)}\frac{x_i^{(N\to cancer)}}{\left|x_i^{(N\to cancer)}\right|}\left(\left|x_i^{(N\to cancer)}\right| - 1\right)\left(1 - p_i^{(N\to cancer)}\right)$$

$$WPR_\Gamma^{(N\to cancer)} = \overline{WIR_i^{(N\to cancer)}}\Big|_{i\in\Gamma}$$

Our software to determine these characteristics from the raw data is described in [75].

5. Conclusions

The main finding of this study is that even equally histopathologically graded cancer nodules from the same tumor have different transcriptomic organizations. This conclusion raises serious concerns about the validity of biomarkers identified through meta-analyses of large populations of cancer stricken and cancer free humans and poses new challenges for the germline genetic testing of prostate cancer patients [76].

Our Genomic Fabric Paradigm offers a personalized genomics alternative to the biomarkers approach to determine the cancer transcriptional identity (e.g. [77]).

Author Contributions: Conceptualization, D.A.I..; methodology, D.A.I. and S.I.; software, D.A.I.; validation, D.A.I. and S.I.; formal analysis, D.A.I.; investigation, S.I.; resources, D.A.I.; data curation, D.A.I. and S.I.; writing—original draft preparation, D.A.I. and S.I.; writing—review and editing, D.A.I. and S.I.; visualization, S.I.; supervision, D.A.I.; project administration, D.A.I.; funding acquisition, D.A.I. Both authors have read and agreed to the published version of the manuscript.

Funding: This research received no external funding. D.A.I. was supported by the Texas A&M University System Chancellor's Research Initiative (CRI) funding for the Radiation Institute for Science and Engineering (RaISE) and the Center for Computational Systems Biology (CCSB) at the Prairie View A&M University.

Institutional Review Board Statement: The study was conducted according to the guidelines of the Declaration of Helsinki. At the time of the experiment (2016), the study was part of Dr. D.A. Iacobas' project approved by the Institutional Review Boards (IRB) of the New York Medical College's (NYMC) and Westchester Medical Center (WMC) Committees for Protection of Human Subjects. The approved IRB (L11,376 from 2 October 2015) granted access to frozen cancer specimens from the WMC Pathology Archives and depersonalized pathology reports, waiving patient's informed consent.

Data Availability Statement: Raw and processed gene expression data were deposited and are publicly accessible at https://www.ncbi.nlm.nih.gov/geo/query/acc.cgi?&acc=GSE133906.

Conflicts of Interest: The authors declare no conflict of interest.

References

1. Harmonized Cancer Datasets Genomic Data Commons Data Portal. Available on line: https://portal.gdc.cancer.gov/ (accessed 02/14.2021))
2. Oncomine Assays for Oncology Research. Available on line : https://www.thermofisher.com/us/en/home/clinical/preclinical-companion-diagnostic-development/oncomine-oncology.html (accessed 02/17/2021)
3. Canexia Health Detecting Mutations in Solid Tumor Tissue. Available on line: https://canexiahealth.com/solution/find-it/ (accessed 02/09/2021)
4. Canexia Health Detecting Mutations in Plasma. Available on line: https://canexiahealth.com/solution/follow-it/ (accessed 02/09/2021)
5. Canexia Health Detect Known and Novel Fusions in Solid Tumors. Available on line: https://canexiahealth.com/solution/fusions/ (accessed 02/09/2021)
6. Myriad Prolaris Prostate Cancer. Available on line: https://prolaris.com/physician-central/ (accessed: 02/09/2021)
7. OncotypeIQ. Available on line: https://www.oncotypeiq.com/en-US/prostate-cancer/patients-and-caregivers/early-stage-gps/why-oncotype-dx-gps (accessed: 02/11/2021)
8. Foundation Medicine. Available online: https://www.foundationmedicine.com/genomic-testing (accessed on 12 July 2020).
9. Prostate Cancer is Manageable. Available on line: https://decipherbio.com/ (accessed: 02/08/2021)
10. Emami, N.C.; Cavazos, T.B.; Rashkin, S.R.; Graff, R.E.; Tai, C.G.; Mefford, J.A.; Kachuri, L.; Cario, C.L.; Wan, E.; Wong, S. et al. A large-scale association study detects novel rare variants, risk genes, functional elements, and polygenic architecture of prostate cancer susceptibility. *Cancer Res*. **2020**: canres.2635.2020. doi: 10.1158/0008-5472.CAN-20-2635.
11. Bruinsma, S.M.; Nieboer, D.; Roobol, M.J.; Bangma, C.H.; Verbeek, J.F.M.; Gnanapragasam, V.; Van Hemelrijck, M.; Frydenberg, M.; Lee, L.S.; Valdagni, R. et al. Risk-Based Selection for Active Surveillance: Results of the Movember Foundation's Global Action Plan Prostate Cancer Active Surveillance (GAP3) Initiative. *J Urol*. **2021** doi: 10.1097/JU.0000000000001700. Epub ahead of print.
12. Soo, A.; O'Callaghan, M.E.; Kopsaftis, T.; Vatandoust, S.; Moretti, K.; Kichenadasse, G. PSA response to antiandrogen withdrawal: a systematic review and meta-analysis. *Prostate Cancer Prostatic Dis*. **2021**. doi: 10.1038/s41391-021-00337-0. Epub ahead of print.
13. Forsythe, A.; Zhang, W.; Phillip Strauss, U.; Fellous, M.; Korei, M.; Keating, K. A systematic review and meta-analysis of neurotrophic tyrosine receptor kinase gene fusion frequencies in solid tumors. *Ther Adv Med Oncol*. **2020**; 12:1758835920975613. doi: 10.1177/1758835920975613.
14. Han, F.F.; Ren, L.L.; Xuan, L.L.; Lv, Y.L.; Liu, H.; Gong, L.L.; An, Z.L.; Liu, L.H. HSD3B1 variant and androgen-deprivation therapy outcome in prostate cancer. *Cancer Chemother Pharmacol*. **2021**; 87(1):103-112. doi: 10.1007/s00280-020-04192-z. Epub 2020 Nov 3.

15. Urabe, F.; Kimura, S.; Yamamoto, S.; Tashiro, K.; Kimura, T.; Egawa, S. Impact of family history on oncological outcomes in primary therapy for localized prostate cancer patients: a systematic review and meta-analysis. *Prostate Cancer Prostatic Dis*. **2021**. doi: 10.1038/s41391-021-00329-0. Epub ahead of print.
16. Iacobas, S.; Iacobas, D.A.; Spray, D.C.; Scemes, E. The connexin43 transcriptome during brain development: Importance of genetic background. *Brain Res.* **2012**, *1487*, 131–139, doi:10.1016/j.brainres.2012.05.062.
17. Thomas, N.M.; Jasmin, J.F.; Lisanti, M.P.; Iacobas, D.A. Sex differences in expression and subcellular localization of heart rhythm determinant proteins. *Biochem. Biophys. Res. Commun.* **2011**, *406*, 117–122, doi:10.1016/j.bbrc.2011.02.006.
18. Iacobas, D.A.; Fan, C.; Iacobas, S.; Spray, D.C.; Haddad, G.G. Transcriptomic changes in developing kidney exposed to chronic hypoxia. *Biochem. Biophys. Res. Commun.* **2006**, *349*, 329–338, doi:10.1016/j.bbrc.2006.08.056.
19. Iacobas, D.A.; Iacobas, S.; Nebieridze, N.; Velíšek, L.; Velíšková, J. Estrogen Protects Neurotransmission Transcriptome during Status Epilepticus. *Front. Neurosci.* **2018**, *12*, 332, doi:10.3389/fnins.2018.00332.
20. Desruisseaux, M.; Iacobas, D.A.; Iacobas, S.; Mukherjee, S.; Weiss, L.M.; Tanowitz, H.B.; Spray, D.C. Alterations in the Brain Transcriptome in Plasmodium Berghei ANKA Infected Mice. *J. Neuroparasitol.* **2010**, *1*, 74–81, doi:10.4303/jnp/n100803.
21. Iacobas, D.A.; Chachua, T.; Iacobas, S.; Benson, M.J.; Borges, K.; Velísková, J.; Velísek, L. ACTH and PMX53 recover the normal synaptic transcriptome in a rat model of infantile spasms. *Sci. Rep.* **2018**, *8*, 5722, doi:10.1038/s41598-018-24013-x.
22. Fan, C.; Iacobas, D.A.; Zhou, D.; Chen, Q.; Gavrialov, O.; Haddad, G.G. Gene expression and phenotypic characterization of mouse heart after chronic constant and intermittent hypoxia. *Physiol. Genom.* **2005**, *22*, 292–307, doi:10.1152/physiolgenomics.00217.2004.
23. Thi, M.M.; Iacobas, D.A.; Iacobas, S.; Spray, D.C. Fluid Shear Stress Regulates Vascular Endothelial Growth Factor Gene in Osteoblasts. *Ann. N. Y. Acad. Sci.* **2007**, *1117*, 73–81, doi:10.1196/annals.1402.020.
24. Kobets, T.; Iatropoulos, M.J.; Duan, J.D.; Brunnemann, K.D.; Iacobas, D.A.; Iacobas, S.; Vock, E.; Deschl, U.; Williams, G.M. Effects of Nitrosamines on the Expression of Genes Involved in Xenobiotic Metabolism in the Chicken Egg Alternative Genotoxicity Model. *Toxicol. Sci.* **2018**, *166*, 82–96, doi:10.1093/toxsci/kfy197.
25. Lee, P.R.; Cohen, J.E.; Iacobas, D.A.; Iacobas, S.; Fields, R.D. Gene networks activated by pattern-specific generation of action potentials in dorsal root ganglia neurons. *Sci. Rep.* **2017**, *7*, 43765, doi:10.1038/srep43765.
26. Liu, Y.; Weber, Z.; San Lucas, F.A.; Deshpande, A.; Jakubek, Y.A.; Sulaiman, R.; Fagerness, M.; Flier, N.; Sulaiman, J.; Davis, C.M. et al. Assessing inter-component heterogeneity of biphasic uterine carcinosarcomas. *Gynecol Oncol* **2018**; *151*(2): 243-249 doi: 10.1016/j.ygyno.2018.08.043
27. Fujimoto, H.; Saito, Y.; Ohuchida, K.; Kawakami, E.; Fujiki, S.; Watanabe, T.; Ono, R.; Kaneko, A.; Takagi, S.; Najima, Y. et al. Deregulated Mucosal Immune Surveillance through Gut-Associated Regulatory T Cells and PD-1+ T Cells in Human Colorectal Cancer. *J Immunol* **2018**; *200*(9): 3291-3303 doi: 10.4049/jimmunol.1701222]
28. Yang, C.; Gong, J.; Xu, W.; Liu, Z.; Cui, D. Next-generation sequencing identified somatic alterations that may underlie the etiology of Chinese papillary thyroid carcinoma. *Eur J Cancer Prev* **2019**; DOI: 10.1097/CEJ.0000000000000529
29. Iacobas, D.A. Powerful quantifiers for cancer transcriptomics. World J. Clin. Oncol. **2020**, *11*, 679–704. doi:10.5306/wjco.v11.i9.679.
30. Iacobas, D.A.; Mgbemena, V.E.; Iacobas, S.; Menezes, K.M.; Wang, H.; Saganti, P.B. Genomic Fabric Remodeling in Metastatic Clear Cell Renal Cell Carcinoma (ccRCC): A New Paradigm and Proposal for a Personalized Gene Therapy Approach. *Cancers* **2020**; *12*(12) 3678. DOI: 10.3390/cancers12123678.
31. Kyoto Encyclopedia of Genes and Genomes. Available of line: https://www.kegg.jp (accessed 02/14/2021)
32. Prostate cancer. Available on line: https://www.genome.jp/kegg-bin/show_pathway?hsa05215 (accessed: 01/20/2021)
33. Iacobas, S.; Thomas, N.M.; Iacobas, D.A. Plasticity of the myelination genomic fabric. *Mol Genet Genomics* **2012**; *287*:237-246. https://doi.org/10.1007/s00438-012-0673-0.
34. Iacobas, D.A.; Iacobas, S.; Lee, P.R.; Cohen, J.E.; Fields, R.D. Coordinated Activity of Transcriptional Networks Responding to the Pattern of Action Potential Firing in Neurons. *Genes* (Basel) **2019**, 10, 754. doi: 10.3390/genes10100754
35. Iacobas DA**,** Wen J, Iacobas S, Schwartz N, Putterman C (2021) Remodeling of Neurotransmission, PI3K-AKT and Chemokine Signaling Genomic Fabrics in Neuropsychiatric Systemic Lupus Erythematosus, *Genes (Basel)* **12**(2):251. https://doi.org/10.3390/genes12020251.
36. Apoptosis pathway. Available on line: https://www.genome.jp/kegg-bin/show_pathway?hsa04210 (accessed 02/20/2021)
37. P53 signaling pathway. Available on line: https://www.genome.jp/kegg-bin/show_pathway?hsa04115 (accessed: 02/20/2021)
38. Pathways in cancer. Available on line: https://www.genome.jp/kegg-bin/show_pathway?hsa05200 (accessed: 02/20/2021)
39. Gene Commanding Height (GCH) hierarchy in the cancer nucleus and cancer-free resection margins from a surgically removed prostatic adenocarcinoma of a 65y old black man. Available on line: https://www.ncbi.nlm.nih.gov/geo/query/acc.cgi?&acc=GSE133906 (accessed 02/01/2021)
40. To be provided prior to publication

41. Victorino, P.H.; Marra, C.; Iacobas, D.A.; Iacobas, S.; Spray, D.C.; Linden, R.; Adesse, D.; Petrs-Silva, H. Optic Nerve Crush Activates the Genomic Fabrics of the Complement Cascade and Delta-Notch Signaling. *Genes (Basel)* **2021**; ??
42. Boerrigter, E.; Benoist, G.E.; van Oort, I.M.; Verhaegh, G.W.; van Hooij, O.; Groen, L.; Smit, F.; Oving, I.M.; de Mol, P.; Smilde, T.J. et al. Liquid biopsy reveals KLK3 mRNA as a prognostic marker for progression free survival in patients with metastatic castration-resistant prostate cancer undergoing first-line abiraterone acetate and prednisone treatment. *Mol Oncol*. **2021**. doi: 10.1002/1878-0261.12933. Epub ahead of print.
43. Wang, L.; Li, C.; Tian, J.; Liu, J.; Zhao, Y.; Yi, Y.; Zhang, Y.; Han, J.; Pan, C.; Liu, S. et al. Genome-wide transcriptional analysis of Aristolochia manshuriensis induced gastric carcinoma. *Pharm Biol*. **2020**; *58*(1):98-106. doi: 10.1080/13880209.2019.1710219.
44. Wang ,Z.; Zhong, M.; Song, Q.; Pascal, L.E.; Yang, Z.; Wu, Z.; Wang, K.; Wang, Z. Anti-apoptotic factor Birc3 is up-regulated by ELL2 knockdown and stimulates proliferation in LNCaP cells. *Am J Clin Exp Urol*. **2019**; *7*(4):223-231. PMID: 31511829; PMCID: PMC6734035.
45. Ren, K.; Gou, X.; Xiao, M.; He, W.; Kang, J. Pim-2 Cooperates with Downstream Factor XIAP to Inhibit Apoptosis and Intensify Malignant Grade in Prostate Cancer. *Pathol Oncol Res*. **2019**; *25*(1):341-348. doi: 10.1007/s12253-017-0353-9.
46. Patel, P.G.; Wessel, T.; Kawashima, A.; Okello, J.B.A.; Jamaspishvili, T.; Guérard, K.P.; Lee, L.; Lee, A.Y.; How, N.E.; Dion, D. et al. A three-gene DNA methylation biomarker accurately classifies early stage prostate cancer. *Prostate*. **2019**; *79*(14):1705-1714. doi: 10.1002/pros.23895.
47. Zhang, H.; Zhao, B.; Zhai, Z.G.; Zheng, J.D.; Wang, Y.K.; Zhao, Y.Y. Expression and clinical significance of MMP-9 and P53 in lung cancer. *Eur Rev Med Pharmacol Sci*. **2021**; 25(3):1358-1365. doi: 10.26355/eurrev_202102_24844.
48. Gallazzi, M.; Baci, D.; Mortara, L.; Bosi, A.; Buono, G.; Naselli, A.; Guarneri, A.; Dehò, F.; Capogrosso, P.; Albini, A. et al. Prostate Cancer Peripheral Blood NK Cells Show Enhanced CD9, CD49a, CXCR4, CXCL8, MMP-9 Production and Secrete Monocyte-Recruiting and Polarizing Factors. *Front Immunol*. **2021**; 11:586126. doi: 10.3389/fimmu.2020.586126.
49. Su, B.; Zhang, L.; Zhuang, W.; Zhang, W.; Chen, X. Knockout of Akt1/2 suppresses the metastasis of human prostate cancer cells CWR22rv1 in vitro and in vivo. *J Cell Mol Med*. **2021**; *25*(3):1546-1553. doi: 10.1111/jcmm.16246.
50. Iacobas, D.A.; Iacobas, S., Spray, D.C. Connexin-dependent transcellular transcriptomic networks in mouse brain. *Prog Biophys Mol Biol*. **2007**; *94*(1-2):168-184. Review. DOI:10.1016/j.pbiomolbio.2007.03.015.
51. Iacobas, S.; Amuzescu, B.; Iacobas, D.A. Transcriptomic uniqueness and commonality of the ion channels and transporters in the four heart chambers. *Sci Rep*. **2021**; *11*(1): 2743**.** DOI : 10.1038/s41598-021-82383-1.
52. Rossini, A.; Giussani, M.; Ripamonti, F.; Aiello, P.; Regondi, V.; Balsari, A.; Triulzi, T.; Tagliabue, E. Combined targeting of EGFR and HER2 against prostate cancer stem cells. *Cancer Biol Ther*. **2020**; *21*(5):463-475. doi: 10.1080/15384047.2020.1727702.
53. Iacobas, D.A.; Iacobas, S.; Stout, R.; Spray, D.C. Cellular environment remodels the genomic fabrics of functional pathways in astrocytes. *Genes (Basel)* **2020**; *11*(5), 520; PMID: 32392822, doi: 10.3390/genes11050520.
54. Qiu, X.; Guo, D.; Du, J.; Bai, Y.; Wang, F. A novel biomarker, MRPS12 functions as a potential oncogene in ovarian cancer and is a promising prognostic candidate. *Medicine (Baltimore)*. **2021**; *100*(8):e24898. doi: 10.1097/MD.0000000000024898.
55. Lopes LO, Maués JH, Ferreira-Fernandes H, Yoshioka FK, Júnior SCS, Santos AR, Ribeiro HF, Rey JA, Soares PC, Burbano RR et al. New prognostic markers revealed by RNA-Seq transcriptome analysis after MYC silencing in a metastatic gastric cancer cell line. *Oncotarget*. **2019**; *10*(56):5768-5779. doi: 10.18632/oncotarget.27208.
56. Wu, C.; Rao, X.; Lin, W. Immune landscape and a promising immune prognostic model associated with TP53 in early-stage lung adenocarcinoma. *Cancer Med*. **2021**; *10*(3):806-823. doi: 10.1002/cam4.3655.
57. Cui, L.; Xue, H.; Wen, Z.; Lu, Z.; Liu, Y, Zhang, Y. Prognostic roles of metabolic reprogramming-associated genes in patients with hepatocellular carcinoma. *Aging* (Albany NY). **2020**; *12*(21):22199-22219. doi: 10.18632/aging.104122.
58. Ye S, Lawlor MA, Rivera-Reyes A, Egolf S, Chor S, Pak K, Ciotti GE, Lee AC, Marino GE, Shah J. et al. YAP1-Mediated Suppression of USP31 Enhances NFκB Activity to Promote Sarcomagenesis. *Cancer Res*. **2018**; *78*(10):2705-2720. doi: 10.1158/0008-5472.CAN-17-4052.
59. Haider, S.; Wang, J.; Nagano, A.; Desai, A.; Arumugam, P.; Dumartin, L.; Fitzgibbon, J.; Hagemann, T.; Marshall, J.F.; Kocher, H.M. et al. A multi-gene signature predicts outcome in patients with pancreatic ductal adenocarcinoma. *Genome Med*. **2014**; *6*(12):105. doi: 10.1186/s13073-014-0105-3.
60. Okita, Y.; Kimura, M.; Xie, R.; Chen, C.; Shen, L.T.; Kojima, Y.; Suzuki, H.; Muratani, M.; Saitoh, M.; Semba, K. et al. The transcription factor MAFK induces EMT and malignant progression of triple-negative breast cancer cells through its target GPNMB. *Sci Signal*. **2017**; *10*(474):eaak9397. doi: 10.1126/scisignal.aak9397.
61. Park JS, Pierorazio PM, Lee JH, Lee HJ, Lim YS, Jang WS, Kim J, Lee SH, Rha KH, Cho NH, Ham WS. Gene Expression Analysis of Aggressive Clinical T1 Stage Clear Cell Renal Cell Carcinoma for Identifying Potential Diagnostic and Prognostic Biomarkers. Cancers (Basel). 2020 Jan 16;12(1):222. doi: 10.3390/cancers12010222.
62. Wang, Y.X.; Wang, D.Y.; Guo, Y.C.; Guo, J. Zyxin: a mechanotransductor to regulate gene expression. *Eur Rev Med Pharmacol Sci*. **2019**; *23*(1):413-425. doi: 10.26355/eurrev_201901_16790.
63. Shi, Z.; Wu, D.; Tang, R.; Li, X.; Chen, R.; Xue, S.; Zhang, C.; Sun, X. Silencing of HMGA2 promotes apoptosis and inhibits migration and invasion of prostate cancer cells. *J Biosci*. **2016**; *41*(2):229-36. doi: 10.1007/s12038-016-9603-3.
64. Jamaspishvili, T.; Scorilas, A.; Kral, M.; Khomeriki, I.; Kurfurstova, D.; Kolar, Z.; Bouchal, J. Immunohistochemical localization and analysis of kallikrein-related peptidase 7 and 11 expression in paired cancer and benign foci in prostate cancer patients. *Neoplasma*. **2011**; *58*(4):298-303.

65. Lan, Y.; Hu, X.; Jiang, K.; Yuan, W.; Zheng, F.; Chen, H. Significance of the detection of TIM-3 and FOXJ1 in prostate cancer. *J BUON*. **2017**; *22*(4):1017-1021. PMID: 28952222.
66. Ozturk, K.; Onal, M.S.; Efiloglu, O.; Nikerel, E.; Yildirim, A.; Telci, D. Association of 5'UTR polymorphism of secretory phospholipase A2 group IIA (PLA2G2A) gene with prostate cancer metastasis. *Gene*. **2020**; 742:144589. doi: 10.1016/j.gene.2020.144589.
67. Xia, Z.N.; Wang, X.Y.; Cai, L.C.; Jian, W.G.; Zhang, C. IGLL5 is correlated with tumor-infiltrating immune cells in clear cell renal cell carcinoma. *FEBS Open Bio*. **2021**; *11*(3):898-910. doi: 10.1002/2211-5463.13085.
68. Qian, X.; Li, C.; Pang, B.; Xue, M.; Wang, J.; Zhou, J. Spondin-2 (SPON2), a more prostate-cancer-specific diagnostic biomarker. *PLoS One*. **2012**; *7*(5):e37225. doi: 10.1371/journal.pone.0037225.
69. Josefsson, A.; Larsson, K.; Freyhult, E.; Damber, J.E.; Welén, K. Gene Expression Alterations during Development of Castration-Resistant Prostate Cancer Are Detected in Circulating Tumor Cells. *Cancers* (Basel). **2019**; *12(*1):39. doi: 10.3390/cancers12010039.
70. Liu, T.; Ma, Y.; Wang, Z.; Zhang, W.; Yang, X. Siva 1 Inhibits Cervical Cancer Progression and Its Clinical Prognosis Significance. *Cancer Manag Res*. **2020**; *12*:303-311. doi: 10.2147/CMAR.S232994.
71. Iacobas, D.A.; Iacobas, S.; Spray, D.C. Connexin43 and the brain transcriptome of newborn mice. *Genomics* **2007**. *89*(1), 113-123. DOI:10.1016/j.ygeno.2006.09.007.
72. Agilent-026652 Whole Human Genome Microarray 4x44K v2. Probing sequences available online: https://www.ncbi.nlm.nih.gov/geo/query/acc.cgi?acc=GPL13497 (accessed on 02/12/2020)
73. Iacobas, D.A.; Tuli, N.; Iacobas, S.; Rasamny, J.K.; Moscatello, A.; Geliebter, J.; Tiwari, R.M. Gene master regulators of papillary and anaplastic thyroid cancer phenotypes. *Oncotarget* **2018**; *9*(2), 2410-2424. doi: 10.18632/oncotarget.23417.
74. Iacobas, D.A.; Iacobas, S.; Nebieridze, N.; Velisek, L.; Veliskova, J. Estrogen protects neurotransmission transcriptome during status epilepticus, *Front Neurosci*. **2018**; *12*:332. DOI: 10.3389/fnins.2018.00332.
75. Iacobas, S.; Ede, N.; Iacobas, D.A. The Gene Master Regulators (GMR) Approach Provides Legitimate Targets for Personalized, Time-Sensitive Cancer Gene Therapy. *Genes (Basel)* **2019**; *10*(8), 560. doi:10.3390/genes10080560.
76. Szymaniak, B.M.; Facchini, L.A.; Giri, V.N.; Antonarakis, E.S.; Beer, T.M.; Carlo, M.I.; Danila, D.C.; Dhawan, M.; George, D.; Graff, J.N. Et al. Practical Considerations and Challenges for Germline Genetic Testing in Patients With Prostate Cancer: Recommendations From the Germline Genetics Working Group of the PCCTC. *JCO Oncol Pract*. **2020**; *16*(12):811-819. doi: 10.1200/OP.20.00431.
77. Paull, E.O.; Aytes, A.; Jones, S.J.; Subramaniam, P.S.; Giorgi, F.M.; Douglass, E.F.; Tagore, S.; Chu, B.; Vasciaveo, A.; Zheng, S. et al. A modular master regulator landscape controls cancer transcriptional identity. *Cell*. **2021**; *184*(2):334-351.e20. doi: 10.1016/j.cell.2020.11.045.